

1 Atmospheric black carbon and sulfate concentrations in Northeast 2 Greenland

3

4 A. Massling^{1,2}, I. E. Nielsen^{1,2}, D. Kristensen¹, J. H. Christensen¹, L. L. Sørensen², B. Jensen¹, Q. T.
5 Nguyen³, J.K. Nøjgaard^{1,2}, M. Glasius^{3,4}, H. Skov^{1,2,5}

6

7 ¹Department of Environmental Science, Aarhus University, 4000 Roskilde, Denmark

8 ²Arctic Research Centre, Aarhus University, 8000 Aarhus, Denmark

9 ³Department of Chemistry, Aarhus University, 8000 Aarhus, Denmark

10 ⁴Interdisciplinary Nanoscience Centre, Aarhus University, 8000 Aarhus, Denmark

11 ⁵Institute of Chemical Engineering and Biotechnology and Environmental Technology, University
12 of Southern Denmark, 5230 Odense, Denmark

13

14 Abstract

15 Measurements of Equivalent Black Carbon (EBC) in aerosols at the high Arctic field site Villum
16 Research Station (VRS) at Station Nord in North Greenland showed a seasonal variation in EBC
17 concentrations with a maximum in winter and spring at ground level. Average measured
18 concentrations were about 0.067 +/- 0.071 for the winter and 0.011 +/- 0.009 for the summer period.
19 The data was obtained using a Multi Angle Absorption Photometer (MAAP). A similar seasonal
20 pattern was found for sulfate concentrations with a maximum level during winter and spring
21 analyzed by ion chromatography. Here, measured average concentrations were about 0.485 +/-
22 0.397 for the winter and 0.112 +/- 0.072 for the summer period. A correlation between EBC and
23 sulfate concentrations was observed over the years 2011 to 2013 stating a correlation coefficient of
24 $R^2 = 0.72$. This finding gives the hint that most likely transport of primary emitted BC particles to
25 the Arctic was accompanied by aging of the aerosols through condensational processes. BC and
26 sulfate are known to have only partly similar sources with respect to their transport pathways when
27 reaching the high Arctic. Aging processes may have led to the formation of secondary inorganic
28 matter and further transport of BC particles as cloud processing and further washout of particles is
29 less likely based on the typically observed transport patterns of air masses arriving at VRS.
30 Additionally, concentrations of EC (elemental carbon) based on a thermo-optical method were
31 determined and compared to EBC measurements. EBC measurements were generally higher, but a
32 correlation between EC and EBC resulted in a correlation coefficient of $R^2 = 0.64$.
33 Model estimates of the climate forcing due to BC in the Arctic are based on contributions of long-
34 range transported BC during spring and summer. The measured concentrations were here compared
35 with model results obtained by the Danish Hemispheric Model, DEHM. Good agreement between
36 measured and modeled concentrations of both EBC/BC and sulfate was observed. Also, the
37 correlation between BC and sulfate concentrations was confirmed based on the model results
38 observed over the years 2011 to 2013 stating a correlation coefficient of $R^2 = 0.74$. The dominant
39 source is found to be combustion of fossil fuel with biomass burning as a minor though significant
40 source.

41

42 **1. Introduction**

43 Black carbon (BC) is a component of the atmospheric aerosol, which originates from incomplete
44 combustion of fossil fuels or waste, flaring or natural and anthropogenic biomass burning (Roberts
45 and Jones, 2004; Stohl et al., 2013; Yttri et al., 2014). Long-range transported BC to the Arctic is an
46 important atmospheric component as it contributes to Arctic haze, which has a significant influence
47 on the Arctic radiation budget (Quinn et al., 2008; Hirdmann et al., 2010; Flanner et al., 2007; Wang
48 et al. 2011).

49 BC particles and especially aged BC particles affect the radiation budget directly by scattering and
50 absorbing incoming solar radiation. In case of haze situations the energy can be re-emitted via long-
51 wave radiation (Lubin and Simpson, 1994). In summary, this results in a heating effect below and
52 within the polluted aerosol layer (e.g. AMAP report, 2011). As primary BC particles are
53 hydrophobic, their cloud condensation nucleus activity is very limited unless they do appear in very
54 large sizes. Particles of inorganic matter have much better potential to act as cloud condensation
55 nuclei (CCN). Nevertheless, after a certain degree of chemical aging BC particles may have taken
56 up inorganic matter and such coating can lead to modified particles with sufficient CCN activity. In
57 this way, aged BC particles may also affect the radiation budget indirectly by acting as CCN or ice
58 nuclei (IN) and thereby they may change cloud albedo (Koehler et al., 2009). In addition, deposited
59 BC particles on snow- or ice-covered surfaces have a heating effect in the lower atmosphere due to
60 a lowering of the surface albedo (Quinn et al., 2008; Wang et al., 2011). Such an effect is estimated
61 to cause more rapid melting in the Arctic (Quinn et al., 2008).

62 Sulfate is another important component of the atmospheric aerosol. Sulfate particles are very
63 efficient in scattering incoming solar radiation resulting in a cooling effect (Crutzen, 2006). These
64 particles are also highly associated with aging processes as they appear as secondary inorganic
65 aerosols, e.g. as $(\text{NH}_4)_2\text{SO}_4$ or NH_4HSO_4 (Seinfeld and Pandis, 2006). Furthermore, inorganic
66 sulfate can react with organic aerosol species to form organosulfates (Liggio and Li, 2006; Surratt et
67 al., 2007), which have also been observed in the Arctic (Hansen et al., 2014). The presence of
68 sulfate also enhances the CCN activity in atmospheric aerosol samples (Quinn and Bates, 2011).
69 Sulfate aerosol plays a major role in the Arctic atmosphere because of the climate impact through
70 the scattering effect and cloud forming potential. It has previously been shown that the sulfate
71 concentrations observed at Villum Research Station (VRS) at Station Nord, North Greenland, are
72 dominated by anthropogenic emissions and to a lesser extent are associated with the emission of sea
73 spray particles (Heidam et al. 2004; Nguyen et al., 2013).

74 Several studies have been conducted to characterize the physico-chemical properties of Arctic haze
75 over the past 30 years (e.g. Heidam et al. 1984, 1999 and 2004; Iversen, 1984; Barrie et al., 1989;
76 Skov et al., 2006). Lately, studies have been motivated by the potentially significant climate effects
77 of BC in the Arctic (Sharma et al., 2004, 2006 and 2013; Quinn et al., 2008; Law and Stohl, 2007;
78 Hirdman et al. 2010; Wang et al. 2011). It is well established that the Arctic winter and spring
79 atmosphere is more heavily impacted by transport of air pollution from lower latitudes compared to
80 summer (Heidam et al. 2004; Law and Stohl, 2007).

81 Recent intercomparisons between model results and measurements of northern hemispheric BC
82 concentrations generally show large discrepancies when simulating the seasonality and magnitude
83 of BC in the Arctic (e.g. Koch et al., 2009; Vignati et al. 2010). However, Huang et al. (2010)
84 demonstrated that a reasonable agreement can be obtained between modeled and measured BC
85 concentrations when focusing in the model on the Arctic.

86 The main focus of this paper is to present the dynamics and the seasonality of equivalent black
87 carbon/black carbon (EBC/BC), elemental carbon (EC) and sulfate concentrations over a period of
88 two years and three months at the high Arctic site VRS at Station Nord, North Greenland. In this
89 study the term EC is applied for measurements based on a thermal-optical method whereas EBC is
90 used for measurements based on a light absorption/optical method (Petzold et al., 2013). For black
91 carbon in general and black carbon results based on model outputs we will use the expression BC.

92 Measured EBC and sulfate and modeled BC and sulfate concentrations are compared and the
93 relation between EBC/BC and sulfate is put into context of possible aging and transport
94 mechanisms, which explain the resulting observations. BC and sulfate (precursors of sulfate) can
95 have common sources (e.g. traffic in areas where fuels are not sulfur-free), but they can also
96 originate from different sources (BC from biomass combustion and sulfate from oceanic emissions).
97 It has to be clarified that measurements reported in this study were made near the surface and that
98 radiative forcing depends on the entire column burden.

99 **2. Sampling site and experimental**

100

101 2.1 VRS at Station Nord

102

103 At the Danish military station - Station Nord in North Greenland (81° 36'N, 16° 40'W, and 24 m
104 above mean sea level (msl)) a monitoring station, Villum Research Station (VRS), for atmospheric
105 measurements is located. The main sampling site during this project is a hut (Flygers hut) situated
106 approximately 2.5 km southeast of the military camp. The hut is equipped with inlets for measuring
107 gases and particles. All measurements presented in this article were carried out at this site except the
108 sampling with a High Volume Sampler used further for elemental carbon (EC) analysis, which is
109 described in more detail in a later section.

110

111 2.2 Instrumentation

112

113 *MAAP (Multi Angle Absorption Photometer)*

114

115 In the period from May 2011 to August 2013, observations of the aerosol light absorption
116 coefficient have been conducted at VRS at Station Nord (Flygers hut) using the Multi Angle
117 Absorption Photometer (MAAP, Model 5012 Thermo Scientific) (described in details in Petzold
118 and Schönlinner, 2004). The instrument was operated with a sample flow of about 1 m³ h⁻¹ and the
119 aerosol light absorption coefficient was measured at a wavelength of $\lambda = 670$ nm. The inlet was
120 used without a size cut-off.

121 Aerosol light absorption coefficients were converted to EBC concentrations using a specific
122 absorption coefficient of 6.6 m² g⁻¹, which is a default setting for the MAAP. The specific
123 absorption coefficient is reported to be site-dependent (Petzold et al., 1997, Sharma et al., 2002).
124 The specific absorption coefficient varies strongly with the distance from the source and thus with
125 the aging of the aerosols. We assume that the uncertainty in EBC related to the value of the used
126 specific absorption coefficient can be as large as a factor of 2. According to Petzold et al. (1997) the
127 observed variability ranges from 5 m² g⁻¹ in extremely remote areas to 14 m² g⁻¹ at urban locations
128 and up to 20 m² g⁻¹ at near-street measuring sites in urban areas using an aethalometer operated at a
129 wavelength of 670 nm. A specific absorption coefficient of 10 m² g⁻¹ for the Zeppelin measurement
130 station in Norway, Svalbard (78° 54'N, 11° 53'E, and 478 m above msl) has been reported by Stohl
131 et al. (2007). Also, Sharma et al. (2002) investigated the specific absorption coefficient of BC using
132 a Particle Soot Absorption Photometer (PSAP) and an aethalometer at the Canadian site, Alert, and
133 used a value of about 10 m² g⁻¹ for the PSAP. It was stated that this coefficient tended to decrease at
134 more remote sites among six different sites. Additionally, Sharma et al. (2004) investigated the
135 seasonal variability of the specific attenuation coefficient at Alert, Canada, for an aethalometer
136 operated at a wavelength of 880 nm. A value of 19 m² g⁻¹ was recommended, but he found a
137 seasonal dependence of the value when comparing it with the graphitic content obtained by thermal
138 analysis. In summer a value of about 29 m² g⁻¹ was found. Also, Bond and Bergstrom (2006)
139 reported a value of 7.5 ± 1.2 m² g⁻¹ for freshly emitted (uncoated) soot particles at 550 nm based on
140 a literature review. However, after emission, condensation processes in the atmosphere lead to

141 coating of the BC particles, which can also enhance the absorption of the particles. Based on
142 Andreae and Gelencsér (2006) the specific absorption coefficient for aged BC particles can exceed
143 the value of $7.5 \text{ m}^2 \text{ g}^{-1}$ by a factor of 2. In the light of these findings, a value of $6.6 \text{ m}^2 \text{ g}^{-1}$ for the
144 specific absorption coefficient was used in this study for a high Arctic remote site, although this
145 value may overestimate the equivalent estimated black carbon concentration. This value is the
146 standard value for the MAAP instrument and it was shown that it matches best in different
147 atmospheric environments when using this instrument (Petzold et al., 2002).
148 Because of relatively low EBC concentrations especially during summer, 24 hour data for the
149 MAAP were averaged for weekly samples. Combining the noise level of the instrument and the
150 flow uncertainty in the sample flow, we estimated an overall relative uncertainty of 20 % for EBC
151 concentrations. But this estimate does not include any uncertainty of the specific absorption
152 coefficient as discussed above. Data of black carbon concentrations originating from absorption
153 measurements have rather more to be interpreted with respect to the uncertainty of the specific
154 absorption coefficient. Based on the manufacturer's information we calculated that the detection
155 limit for a 24hour EBC measurements is lower than $0.006 \mu\text{g EBC m}^{-3}$.

156

157 *HVS (High Volume Sampler)*

158

159 EC concentrations at VRS at Station Nord were determined during the same time period, using a
160 Digital DHA 80 high volume sampler (HVS, Digital/Riemer Messtechnik, Germany) for PM_{10} . The
161 high volume sampler was operated at a flow rate of 500 l min^{-1} using 150 mm prebaked quartz fiber
162 filters (Advantec, Japan). The sampling was done in weekly intervals implying 5000 m^3 of air were
163 sampled on each filter. The samples were collected at the military station at the edge of the camp at
164 Station Nord located 2.5 km from the main sampling site (Flygers hut). The location of the high
165 volume sampler has practical reasons. It was first established to measure the long range transport of
166 long lived pesticides where there is not any local sources and because there was not enough power
167 also to run a HVS at Flygers Hut. Pollution from the camp with respect to EC cannot be excluded
168 here, but the data have been included in the analysis as a comparison of different techniques still
169 creates new knowledge on the relationships between EC and EBC. As the data are on weekly
170 average, the data could not be screened for potential local pollution, which might be contributions
171 from ground transport in the camp, some burning of garbish during small time periods, and the
172 landing, taxi and take-off of airplanes on irregular schedule.

173 The carbon analyzer was a thermal-optical OC/EC instrument from Sunset Laboratory Inc. (Tigard,
174 OR, USA). Punches of 2.5 cm^2 were cut from the filters and analyzed according to the EUSAAR-2
175 protocol (Cavalli et al., 2010). Only front filters were available, so it was not possible to correct for
176 possible positive artifacts, where volatile species adsorb to the filter and add to the particulate
177 organic carbon mass. In this regard, OC but not EC may be overestimated and should only be used
178 with great caution. The detection limit of this set up is $0.37 \mu\text{g C}$ for a 2.5 cm^2 filter punch, i.e.
179 $0.0045 \text{ C } \mu\text{g m}^{-3}$ (Birch and Cary, 1996).

180

181 *(FPS) Filter Pack Sampler*

182

183 In addition, weekly aerosol samples were collected at the monitoring station VRS (Flygers hut)
184 using a filter pack sampler (FPS, custom built), which consists of a setup with 8 filterpacks in series
185 which are operated for a week at a time. An additional filter pack is always taken as a blank. The
186 filter pack consists of three individual filters. The first filter collects particles. The subsequent filters
187 are specially impregnated to collect various gases, notably SO_2 . The filter pack is described in detail
188 in Skov et al. (2006) and Heidam et al. (2004). A flow of 40 L min^{-1} was sucked through the filter
189 pack sampler and a total of about 400 m^3 was sampled on a millipore membrane filter made of
190 mixed cellulose esters. The resulting filters were extracted and analyzed for sulfate using ion
191 chromatography. The technique is described in more detail by Heidam et al. (2004). The

192 uncertainty of the measurements far from the detection limits were better than 20% expressed as 2
193 relative standard deviations (Heidam et al. 2004). The detection limit is $0.0015 \mu\text{g S m}^{-3}$ for both
194 sulfate and sulfur dioxide.

195 **3. The Danish Eulerian Hemispheric Model (DEHM)**

196 The transport and transformation of BC and sulfate to the Arctic originating from anthropogenic and
197 natural sources outside the Arctic was simulated by DEHM (Christensen, 1997; Christensen et al.,
198 2004; Heidam et al. 2004, Skov et al. 2006; Hole et al., 2009; Brandt et al., 2012). The model
199 system consists of a weather forecast model the PSU/NCAR (Pennsylvania State University/
200 National Center for Atmospheric Research) Mesoscale Model version 5 (MM5) modeling
201 subsystem (see Grell et al., 1995). This subsystem is driven by global meteorological data from the
202 European Centre for Medium-Range Weather Forecasts (ECMWF) or National Centers for
203 Environmental Prediction (NCEP). The DEHM model includes 2-way nesting capabilities (Frohn et
204 al., 2002).

205 In this study the model was set up with a horizontal resolution of $150 \text{ km} \times 150 \text{ km}$ south of 60° N
206 and a nested grid of $50 \text{ km} \times 50 \text{ km}$ north of 60° N , both model domains with the North Pole in the
207 centre. The vertical resolution was defined on an irregular grid with 29 layers up to approximately
208 15 km reflecting the structure of the atmosphere. The basic chemical scheme in DEHM includes 67
209 different species and is based on the scheme by Strand and Hov (1994). The chemical scheme has
210 been extended with a detailed description of the ammonia chemistry. Furthermore, reactions
211 concerning the wet-phase production of sulfate have been included. The current model describes
212 concentration fields of 58 photo-chemical compounds (including NO_x , SO_x , VOC, NH_x , CO, O_3
213 etc.) and several classes of particulate matter, where one class is related to BC. This class comprises
214 of two types of BC components: freshly emitted BC, which is treated as hydrophobic, and aged
215 coated BC, which is treated as hygroscopic material. The transformation from freshly emitted BC to
216 aged, coated BC was treated linearly in the model with a lifetime of freshly emitted BC set to 24
217 hours. Both BC species and sulfate are assumed to be a bulk representation of the particles by a
218 mean particle diameter of $1 \mu\text{m}$. The anthropogenic emissions used are based on the Representative
219 Concentration Pathways emissions (RCP emissions) with a $0.5^{\circ} \times 0.5^{\circ}$ resolution (Lamarque et al.,
220 2010). These emissions from the EMEP expert database (European Monitoring and Evaluation
221 Programme) are used for the areas over Europe with $50 \text{ km} \times 50 \text{ km}$ resolution (Mareckova et al.,
222 2008). Furthermore, the biomass burning emissions for the years 1997-2010 are based on the Global
223 Fire Emissions Database version 3 (GFED 3) (van der Werf et al., 2010), which have a horizontal
224 resolution of a 0.5×0.5 on a monthly time step. For the model runs after 2010 the GFED 3 emissions
225 for 2010 were used. The calculation of the dry deposition velocity is based on the resistance
226 method. The parameterisation of wet deposition is based on a simple scavenging ratio formulation
227 with in-cloud and below-cloud scavenging coefficients for both gas and particulate phase.

228 There are several uncertainties connected to the model calculations of sulfate and
229 BC which are large and cannot be estimated for this study. The annual averaged anthropogenic
230 emissions of SO_2 and BC were used in the model and these could have an uncertainty of at least
231 20 % on the yearly basis. These yearly emissions are distributed to daily or hourly emissions using
232 simple time profiles resulting in emissions on shorter timescales having larger uncertainties
233 compared to the total yearly emissions. These time profiles are available as data files from the
234 EMEP model website, (www.emep.int), see also Simpson et al., 2012). The seasonal time profiles
235 are only applied for the European countries. Furthermore the emissions from biomass burning have
236 even larger uncertainties compared to the anthropogenic emissions. There are also uncertainties
237 associated with predicted three-dimensional wind fields, clouds, precipitation, and turbulence by the
238 MM5 model, especially in the Arctic due to the limited number of meteorological observations
239 inside the Arctic. These uncertainties of the meteorological fields could have large influence on the
240 total model uncertainties for a transport over several thousand kilometres from sources in mid-

241 latitudes to e.g. VRS at Station Nord. Finally there are several parameterizations inside the transport
242 model, which increase the uncertainties: the simple scavenging by precipitation (snow or rain), the
243 turbulence parameterization and the bulk representation of the particles by a particle diameter of
244 $1\ \mu\text{m}$.

245 **4. Results and Discussion**

246 **4.1. Comparison of EBC and EC concentrations**

247 Time series of weekly EBC and EC concentrations measured at VRS in the period from May 2011
248 to August 2013 are presented in Fig. 1a. The maximum concentration of EBC was about $0.34\ \mu\text{g m}^{-3}$
249 during winter 2012/2013, while the highest EC concentration was found to be $0.13\ \mu\text{g m}^{-3}$ for the
250 same week. Both the EBC and EC weekly minimum concentrations were close to zero. A seasonal
251 variation was observed for EBC and EC with highest concentrations during winter and spring and
252 minimum concentrations during summer.

253 Generally, Fig. 1a shows good agreement between the patterns of EBC and EC concentrations,
254 however EBC concentrations are often higher compared to EC concentrations. Differences between
255 the two parameters are expected since the EC and EBC concentrations are based on two different
256 measurement techniques which both experience several problems due to different artefacts. In Fig.
257 1b, the correlation between EBC and EC is shown resulting in a slope of $y = 0.50$ and a correlation
258 coefficient of $R^2 = 0.64$. In principle, the overestimation of EBC in comparison to EC as observed in
259 the time series is reflected in the correlation plot. A further look into seasonal mean values of EBC
260 and EC shows that this overestimation is more pronounced during the winter and spring period
261 when Arctic haze is observed (Tab. 1). The fraction of OC/EC is almost constant over the seasons
262 and does not give an additional hint that based on specific emissions the fraction of EC might be
263 underestimated for indicative seasons.

264 The EC/OC carbon analyzer used in this study is based on a thermal-optical method, which corrects
265 for charring that may otherwise overestimate EC. However, artifacts may also arise if samples
266 contain brown carbon (BrC), which is a part of organic carbon that absorbs in the visible and
267 ultraviolet spectral regions (Kirchstetter and Novakov, 2004; Andreae and Gelencsér, 2006). BrC
268 can be volatilized over a broad temperature range and some of the BrC can be accounted for as EC,
269 hence overestimating the EC concentration (Andreae and Gelencsér, 2006). Another issue is the fact
270 that the combustion temperature of EC and BrC can be lowered in the presence of inorganic
271 species, which are sampled on the filter and can catalyze the oxidation of EC and BrC (Andreae and
272 Gelencsér, 2006). This can result in misinterpretation of EC as OC and hence lead to an
273 underestimation of the EC mass concentration. From inspection of Fig. 1, an underestimation of EC
274 could possibly influence the results, whereas volatilization of BrC on the cost of organic carbon and
275 thus overestimation of EC is not likely to occur.

276 The difference between EBC and EC concentration could furthermore be explained by the
277 assumption that the measured absorption coefficients by the MAAP is ascribed to EBC. This might
278 not be entirely correct since a minor fraction of the absorption could be caused by BrC (Andreae
279 and Gelencsér, 2006). Therefore, the higher EBC concentration could be explained by a higher
280 content of BrC. Furthermore the default specific absorption coefficient for the MAAP of $6.6\ \text{m}^2\ \text{g}^{-1}$
281 could be too low since previous studies suggest an enhancement of the absorption coefficient of
282 aged aerosols due to coating, which can increase the specific absorption coefficient with a factor of
283 two or more (Andreae and Gelencsér, 2006). This would contribute to an overestimation of the EBC
284 concentration which could help explain the discrepancy between our EBC and EC concentrations.
285 In fact, Petzold et al. (1997) found the specific absorption coefficient varying within a wide range
286 when summarizing published values from a number of different studies including different locations
287 and thus different aging status of the observed aerosol. Additionally, also soil dust is known to have
288 absorbing character (Fialho et al., 2005), which might enhance the estimated EBC concentration
289 when present in the observed aerosol. The MAAP was operated with no size cut-off so that the

290 detection of soil dust cannot be excluded, while the EC measurements had a particle size cut-off of
291 10 μm in diameter.
292 Another explanation for occasionally observed differences could be that measurements of EBC and
293 EC were not being conducted at the exact same location. The HVS, used to sample EC, was located
294 at Station Nord in the military camp whereas the MAAP was installed approximately 2.5 km from
295 the station (“Flygers hut”). This could explain why the EC concentrations occasionally exceed the
296 EBC concentrations since these higher values could originate from local pollution events in the
297 military camp at Station Nord, though it is manned with 5 permanent staffs and consequently has
298 very low emissions.

299 **4.2. Seasonal variation of measured EBC and sulfate concentrations**

300 Figure 2 shows the weekly time series of EBC and sulfate concentrations measured at VRS between
301 May 2011 and August 2013. Sulfate maximum concentrations were up to 1.746 $\mu\text{g m}^{-3}$ for weekly
302 mean values coinciding with the maximum value during the study period of black carbon
303 concentration at about 0.336 $\mu\text{g m}^{-3}$ (only one data point as indicated in Fig. 2). Minimum sulfate
304 concentrations were close to or below the detection limit and appeared simultaneously with the
305 minimum of equivalent black carbon concentrations which were also close or below the detection
306 limit. A clear seasonal pattern was observed for both EBC and sulfate with maximum
307 concentrations in winter/spring and minimum concentrations in summer each year (Fig. 2). The
308 observed pattern for sulfate is identical with previous observations at VRS (Heidam et al., 2004).
309 In comparison, reported BC concentrations from the field stations Alert, Canada (82.5° N 62.3° W,
310 210 m asl), and Zeppelin on Svalbard, Norway (78.9° E, 11.9° E, 478 m asl), exhibit similar seasonal
311 patterns as observed at Station Nord (AMAP report, 2011; Sharma et al., 2013). At the Alert field
312 station the highest BC concentrations were found to be up to 0.089 $\mu\text{g m}^{-3}$ and at the Zeppelin field
313 station on Svalbard the highest BC concentrations were found up to 0.082 $\mu\text{g m}^{-3}$ during
314 winter/spring 2007/2008. During the following winter/spring (2008/2009) the maximum BC
315 concentration at the Zeppelin field station reached only values up to 0.036 $\mu\text{g m}^{-3}$. This is in good
316 agreement with values found in this study for a later time period regarding the typical winter and
317 spring maximum values.

318 Mean concentrations of measured EBC at VRS during winter (measurement period: December to
319 February) were about 0.067 \pm 0.071 $\mu\text{g m}^{-3}$ compared to the summer (measurement period: June to
320 August) where mean values were about 0.011 \pm 0.009 $\mu\text{g m}^{-3}$. In contrast, the corresponding values
321 for sulfate were 0.485 \pm 0.397 $\mu\text{g m}^{-3}$ for winter and about 0.112 \pm 0.072 $\mu\text{g m}^{-3}$ for summer
322 during the measurement period. The values are also listed in Tab. 1.

323 The ratio between sulfate and EBC is a little lower in autumn and winter compared to spring and
324 summer, but does not give a hint that biomass contribution may have a significant impact on the
325 distribution between sulfate and EBC during special time periods. This is different with regard to
326 the ratio between sulfate and EC where lower values are observed during summer and autumn,
327 which might be indicative for biomass burning during e.g. the summer period as only minor
328 emissions from sulfate are expected from this source compared to black carbon.

329 **4.3. Comparison of measured and modeled EBC/BC and sulfate concentrations**

330 The results of modeled BC and modeled sulfate concentrations from DEHM are presented together
331 with the corresponding measurements of EBC and sulfate observed at VRS in the period from May
332 2011 to August 2013 in Fig. 3a and 3b. The examined EBC/BC and sulfate concentrations exhibit
333 very similar patterns characterized by higher concentrations in winter/spring compared to summer,
334 which is in accordance with the seasonal cycle of Arctic Haze observed in Arctic regions by several
335 authors (Heidam et al., 1984; 1999, 2004; Iversen et al., 1984; Barrie et al., 1989; Stohl et al.,
336 2007).

337 In general, it can be concluded that the seasonal variation of both species is reproduced well by the
338 model. For VRS, the EBC measurements state seasonal mean values which are about a factor of 1.5

339 to 2.5 higher compared with the BC model results during winter and spring. On the other hand the
340 model seems to overestimate the measured sulfate concentrations (seasonal mean values) in
341 autumn, winter, and spring by a factor between 1.3 and 2.3.
342 Discrepancies seen for EBC/BC (Fig. 3a) can be explained by the larger uncertainties of emission
343 inventories used as input for the model of BC compared to emission inventories of sulfur dioxide
344 and sulfate with relation to both the total amount and the temporal and geographical variations.
345 Another important reason for these discrepancies could be due to model inadequacy in the model
346 description of the physics, e.g the bulk external mixed representation of the particles. For example,
347 there is little information known about the daily and seasonal activity pattern concerning BC
348 emissions, which is also reflected in the uncertainty of the emission inventories. Emissions from
349 wild and agricultural fires are calculated based on GFED data (Global Fire Emissions Database) on
350 a monthly basis. Emission events rarely last a month and higher resolution data are urgently
351 required, which is expected to improve the agreement between measured and modeled EBC/BC
352 concentrations.
353 Previous studies comparing measured and modeled values for a 10-year period at Station Nord
354 suggested that DEHM in general describes the sulfate concentrations in the Arctic well (Heidam et
355 al., 1999, 2004; Christensen, 1997) which is also apparent from Fig. 3b. Nevertheless, the model
356 performance for the studied period is not as good as for previous years. The reason for that might be
357 changes in the interannual emissions, which not yet have been incorporated in the model.
358 Measurements of sulfate at VRS show a large decrease of more than a factor of two with respect to
359 the yearly mean concentrations from 2008 to 2012, while the model concentrations have only a
360 small variability (+/- 10-20%). The emissions data in the model were the best available estimate up
361 to date.
362 The seasonality of air pollutants at Station Nord occurs predominantly because of specific transport
363 patterns of air masses, which are highly related to the location and extension of the polar vortex.
364 Thus, transport of pollution into the Arctic boundary layer from mid-latitudes is much more likely
365 in winter and spring compared to summer. These seasonal patterns are well reproduced for EBC/BC
366 and sulfate concentrations by the measurement and model results.
367 Mean concentrations of modeled BC at VRS during winter (December to February) were about
368 $0.040 \pm 0.033 \mu\text{g m}^{-3}$ compared to summer (June to August) where mean values were about
369 $0.019 \pm 0.013 \mu\text{g m}^{-3}$. In contrast, the corresponding modeled values for sulfate in winter were
370 $0.900 \pm 0.657 \mu\text{g m}^{-3}$ and about $0.144 \pm 0.097 \mu\text{g m}^{-3}$ for the summer period. The values are also
371 listed in Tab. 1.
372

373 **4.4. Atmospheric processing of BC and sulfate in the Arctic**

374 Orthogonal regression was applied separately to the measured and modeled data of EBC/BC and
375 sulfate concentrations. The EBC/BC and sulfate concentrations were found to correlate with an R^2
376 correlation coefficient of 0.84 for the measured values (Fig. 4a) and correspond to a value of R^2
377 correlation coefficient of 0.85 for the modeled values (Fig. 4b). Pure BC atmospheric particles are
378 known to be primarily emitted, whereas sulfate aerosol is a combination of minor contributions of
379 primary emitted sulfate aerosol and dominated by secondary inorganic aerosol formation favored by
380 the photo-oxidation of sulfur dioxide. For VRS at Station Nord it has previously been shown that
381 anthropogenic emissions of sulfur dioxide and sulfate is the main source of sulfate aerosol by
382 application of the COstrained Physical REceptor Model (COPREM) and the Danish Eulerian
383 Hemispheric Model (DEHM) (Heidam et al. 2004). The results suggested that photo-oxidation of
384 dimethyl sulfide (DMS) and sea-salt sulfate plays a minor role in winter and spring time. In summer
385 time, the relative contribution from DMS to sulfate might be larger. A recent study by Nguyen et al.
386 (2013) at Station Nord (VRS) also suggests that sulfate aerosol and sulfur dioxide predominantly
387 originate from anthropogenic emissions such as Siberian metal smelters and other long-range
388 transported anthropogenic pollution.

389 The positive correlation between EBC/BC and sulfate concentrations at VRS indicates that they
390 undergo a similar transport pattern despite having partly different sources. Also, the simultaneous
391 emission of BC and sulfate favours a positive correlation of the two species at the remote Arctic
392 site. However, BC is known to be emitted in the submicrometer size regime. The particles can either
393 grow by condensation or coagulation and in this way reach sizes around 0.5 μm in aerodynamic
394 diameter where they have the longest atmospheric life times and thus can be transported over the
395 longest distances (Seinfeld and Pandis 2006; Huang et al. 2010). It should be added that BC
396 originated from e.g. biomass combustion is supposed to have sizes of up to a few hundred
397 nanometers in diameter when freshly emitted. BC originated from e. g. traffic is rather more emitted
398 in smaller size ranges of up to about only one hundred nanometer in diameter.
399 Since BC and sulfate are only partly related to the same combustion sources during winter and
400 spring, we hypothesize that sulfate particles function as transport containers for BC matter as the
401 concentration of sulfate is clearly dominating and mostly formed in secondary processes. Although
402 our study does not investigate the state of mixing of observed aerosols, it is most likely that sulfate
403 and BC are internally mixed as BC appears aged only short time after release, which can be
404 indicated by its loss of hydrophobic character (Swietlicki et al., 2008).
405 By comparing the scatter plots of measured (Fig. 4a) and modeled (Fig. 4b) values, it is apparent
406 that the DEHM model for VRS results in similar correlation coefficients between BC and sulfate as
407 observed for the measurements for EBC and sulfate as mentioned above. The slopes of the two
408 correlations $y = 5.86$ (measurement results) and $y = 24.15$ (model results) obtained by orthogonal
409 regression are on the contrary rather different from each other stating that from the perspective of
410 measurement results concentrations of sulfate aerosol are by a factor of about six higher compared
411 to concentrations of black carbon aerosol whereas model results state concentrations of sulfate
412 aerosol are by a factor of 24 higher.
413 Assuming that particles at VRS arrive as internally mixed particles composed of black carbon,
414 sulfate and some other inorganic and organic species, a freshly emitted primary BC particle might
415 experience a substantial diameter growth during long-range transport to the Arctic prolonging its
416 lifetime in relation to dry deposition, because the dry deposition velocity for small particles (50 to
417 100 nm in size) decreases with increasing diameters up to approximately 0.5 μm (Slinn and Slinn,
418 1980; Slinn, 1982) and therewith increasing its probability to reach the Arctic. Also, in general, a
419 low deposition rate is observed during the Arctic winter enhancing the long-range transport of air
420 pollutants.
421 On the other hand, any up-take of soluble material and implied change from hydrophobic to
422 hydrophilic character also enhances the chance of the particle to get involved in a cloud process and
423 thus the chance for wet deposition. But the main pathway in the lower troposphere for Arctic Haze
424 during winter and spring is from sources north of the Arctic Front in northern Eurasia over snow-
425 or ice-covered surfaces (Stohl, 2006; Christensen, 1997). This atmospheric transport is highly
426 episodic and often related to large-scale blocking events over Siberia and with only none or small
427 amount of precipitation events during the transport episodes (Raatz and Shaw, 1984; Christensen,
428 1997). This means even though the increased hydrophilic character of BC tends to decrease the
429 lifetime, the wet deposition is still small during the transport episodes.
430 The described circumstances also indicate that the source areas for BC and SO_2 (precursor for
431 sulfate aerosol) are similar, especially during the winter and spring time and the removal processes
432 of BC and sulfate are also similar to a certain extent.

433 **5. Summary and conclusions**

434 The characteristics of Arctic air pollution with respect to EBC/BC, EC and sulfate aerosol observed
435 at the high Arctic site, Villum Research Station at Station Nord, for a period of two years and three
436 months was investigated in this study to improve our understanding of the particle dynamics in
437 relation to their properties, life times and mutual dependencies.

438 EBC and EC concentrations followed the same pattern, but measured concentrations values of EBC
439 were about a factor of 2 higher which is explained by the limits of the different techniques.
440 Measurements together with model results were used to estimate the concentration levels and the
441 seasonal variation of EBC/BC and sulfate to the Arctic and to understand the interplay of the two
442 species during transport to the Arctic region. Measured EBC concentrations showed average
443 concentrations of $0.067 \mu\text{g m}^{-3}$ in winter and $0.011 \mu\text{g m}^{-3}$ in summer compared to values of 0.485
444 $\mu\text{g m}^{-3}$ in winter and $0.112 \mu\text{g m}^{-3}$ in summer for sulfate. Corresponding modeled values were 0.040
445 $\mu\text{g m}^{-3}$ in winter and $0.019 \mu\text{g m}^{-3}$ in summer for BC and $0.900 \mu\text{g m}^{-3}$ in winter and $0.144 \mu\text{g m}^{-3}$ in
446 summer for sulfate.

447 It was found that EBC/BC and sulfate concentrations exhibit very similar patterns, characterized by
448 higher concentrations in winter/spring compared to summer, which is in accordance with the
449 seasonal cycle of Arctic Haze and its annual variation. This was found in both, measurement and
450 model results.

451 A comparison of measured and modeled concentrations of EBC/BC and sulfate has been carried
452 out. The results show good agreement between the measured and modeled concentrations of both
453 species with respect to their seasonal pattern indicating that the model is able to describe the strong
454 seasonal variation of both BC and sulfate concentrations. Nevertheless, the relationship in mass
455 ratio between sulfate and EBC/BC is observed to be much lower for the measurement results
456 compared to the model results. The most likely reason for this discrepancy is the overestimation of
457 modeled sulfate concentrations, which probably is due to changes in the interannual emissions of
458 SO_2 , which not have been included in the used emissions inventories. Model results from earlier
459 years do not show this large overestimation.

460 A specific relationship between sulfate concentrations and EBC/BC was observed for the entire
461 study period. This indicates that both species undergo a common aging process, which
462 predominantly leads to accumulation of BC and sulfate containing particles following the same
463 transport pattern to the high Arctic. Sulfate aerosol seems to function as transport container for BC
464 matter. In this way, particles are composed of a mixture of carbonaceous and inorganic material and
465 reach sizes enhancing their lifetime giving the possibility to be transported over long distances in
466 the atmosphere reaching eventually e.g. the high Arctic. A low deposition rate during the Arctic
467 winter is most likely supporting this process.

468 For more understanding of aerosol aging processes during long-range transport from Eurasia and
469 North America to the Arctic environment it will be highly relevant to get more information on the
470 size segregated chemical composition of Arctic submicrometer aerosols.

471 **Authors` contribution**

472 A. M. prepared the manuscript with contributions from all co-authors. I. E. N. and D.K. analyzed
473 the filters for EC measurements, I. E. N. evaluated the MAAP measurements and provided a
474 literature review for the article. Q. T. N. prepared the instruments for analysis and calibrated those.
475 H. S. and L. L. S. designed the experiments. J. K. N. and M. G. and supervised the data analysis, J.
476 K. N. controlled the carbon analysis . B. J. installed the sampling techniques and carried out the
477 experiments. J. H. C. developed the model code and performed the simulations. All authors have
478 contributed to revising the manuscript and have approved the final version.

479 **Acknowledgement**

480 This work was financially supported by “The Danish Environmental Protection Agency” with
481 means from the MIKA/DANCEA funds for Environmental Support to the Arctic Region. The
482 Nordic Centre of Excellence CRAICC and EU 7th Framework program is acknowledged for
483 financial support. The Royal Danish Air Force is acknowledged for providing free transport to
484 Station Nord, and the staff at Station Nord is especially acknowledged for excellent support. Villum
485 Foundation is acknowledged for the large grant making it possible to build the new research station,

486 Villum Research Station (VRS), at Station Nord.

487

488 **References**

- 489 AMAP report, Arctic Monitoring and Assessment Programme: The Impact of Black Carbon on
490 Arctic Climate, edited by: Quinn, P. K., Stohl, A., Arneth, A., Berntsen, T., Burkhardt, J. F.,
491 Christensen, J., Flanner, M., Kupiainen, K., Lihavainen, H., Shepherd, M., Shevchenko, V.,
492 Skov, H., Vestreng, V., Norwegian Institute for Air Research, Oslo, 72 pp., 2011.
- 493 Andreae, M. O., Gelencsér, A.: Black carbon or brown carbon? The nature of light-absorbing
494 carbonaceous aerosols, *Atmos. Chem. Phys.*, 6, 3131-3148, 2006.
- 495 Barrie, L. A., den Hartog, G., Bottenheim, J. W., Landsberger, S.: Anthropogenic aerosols and gases
496 in the lower troposphere at Alert Canada in April 1086, *J. Atmos. Chem.*, 9 (1-3), 101-127,
497 1989.
- 498 Birch, M. E., Cary, R. A.: Elemental carbon-based method for monitoring occupational exposures to
499 particulate diesel exhaust, *Aero. Sci. and Technol.*, 25 (3), 221-241, 1996.
- 500 Bond, T. C., Bergstrom, R. W.: Light Absorption by Carbonaceous Particles: An Investigative
501 Review, *Aero. Sci. Technol.*, 40, 27-67, 2006.
- 502 Brandt, J., Silver, J. D., Frohn, L. M., Geels, C., Gross, A., Hansen, A. B., Hansen, K. M.,
503 Hedegaard, G. B., Skjøth, C. A. Villadsen, H., Zare, A., Christensen, J. H.: An integrated
504 model study for Europe and North America using the Danish Eulerian Hemispheric Model
505 with focus on intercontinental transport, *Atmos. Environ.*, 53, 156-176, 2012.
- 506 Cavalli, F., Viana, M., Yttri, K. E., Genberg, J., Putaud, J.-P.: Toward a standardised thermal-optical
507 protocol for measuring atmospheric organic and elemental carbon: the EUSAAR protocol,
508 *Atmos. Meas. Tech.*, 3, 79-89, 2010.
- 509 Christensen, J. H.: The Danish Eulerian hemispheric model - A three-dimensional air pollution
510 model used for the Arctic, *Atmos. Environ.*, 31, 4169-4191, 1997.
- 511 Christensen, J. H., Brandt, J., Frohn, L. M., Skov, H.: Modelling of mercury in the Arctic with the
512 Danish Eulerian Hemispheric Model, *Atmos. Chem. and Phys.*, 4, 2251-2257, 2004.
- 513 Crutzen, P.: Albedo enhancement by stratospheric sulfur injections: A contribution to resolve a
514 policy dilemma?, *Climatic change*, 77 (3-4), 211-219, 2006.
- 515 Fialho, P., Hansen, A. D. A., Honrath, R. E.: Absorption coefficients by aerosols in remote areas: a
516 new approach to decouple dust and black carbon absorption coefficients using seven-
517 wavelength Aethalometer data, *J. Aerosol Sci.*, 36, 267-282, 2005.
- 518 Flanner, M. G., Zender, C. S., Randerson, J. T., Rasch, P. J.: Present-day climate forcing and
519 response from black carbon in snow, 112, D11202, doi: 10.1029/2006JD008003, 2007.
- 520 Frohn, L. M., Christensen, J. H.; Brandt, J.: Development of a high-resolution nested air pollution
521 model - The numerical approach, *J. Comput. Phys.*, 179 (1), 68-94, 2002.
- 522 Grell, G. A., Dudhia J., Stauffer D. R.: A Description of the Fifth-Generation Penn State/NCAR
523 Mesoscale Model (MM5), NCAR/TN-398+STR. NCAR Technical Note, Mesoscale and
524 Microscale Meteorology Division, National Center for Atmospheric Research, Boulder,
525 Colorado, 122 pp., 1995.
- 526 Hansen, A.M.K. , Kristensen, K., Nguyen, Q.T., Zare, A., Cozzi, F., Nøjgaard, J.K., Skov, H.,
527 Christensen, J., Brandt, J., Ström, J., Tunved, P., Krejci, R., Glasius, M: Identification of
528 organosulfates and organic acids in Arctic aerosols: Speciation, annual variation and
529 concentration levels, *Atmos. Chem. Phys.*, 14, 7807-7823, 2014.
- 530 Heidam, N. Z.: The Components of the Arctic Aerosol, *Atmos. Environ.*, 18, 329-343, 1984.
- 531 Heidam, N. Z., Christensen, J., Wählin, P., Skov, H.: Arctic atmospheric contaminants in NE
532 Greenland: levels, variations, origins, transport, transformations and trends 1990-2001, *Sci.*
533 *Tot. Environ.*, 331, 5-28, 2004.
- 534 Heidam, N. Z., Wählin, P., Christensen, J. H.: Tropospheric gases and aerosols in northeast

535 Greenland, *J. Atmos. Sci.*, 56, 261-278, 1999.

536 Hirdman, D., Burkhardt, J. F., Sodemann, H., Eckhardt, S., Jefferson, A., Quinn, P. K., Sharma, S.,
537 Strom, J., Stohl, A.: Long-term trends of black carbon and sulphate aerosol in the Arctic:
538 changes in atmospheric transport and source region emissions, *Atmos. Chem. and Phys.*, 10,
539 9351-9368, 2010.

540 Hole, L.R., Christensen, J.H., Ruoho-Airola, T., Tørseth, K., Ginzburg, V., Glowacki, P.: Past and
541 future trends in concentrations of sulphur and nitrogen compounds in the Arctic, *Atmos.*
542 *Environ.*, 43 (4), 928-939, 2009.

543 Huang, L., Gong, S. L., Jia, C. Q., Lavoue, D.: Importance of deposition processes in simulating the
544 seasonality of the Arctic black carbon aerosol, *J. Geophys. Res.*, 115, doi:
545 10.1029/2009JD013478, 2010.

546 Iversen, T.: On the Atmospheric Transport of Pollution to the Arctic, *Geophys. Res. Lett.*, 11, 457-
547 460, 1984.

548 Kirchstetter, T. W., Novakov, T., and Hobbs, P. V.: Evidence that the spectral dependence of light
549 absorption by aerosols is affected by organic, *J. Geophys. Res.*, 109, doi:
550 10.1029/2004JD004999, 2004

551 Koch, D., Schulz, M., Kinne, S., McNaughton, C., Spackman, J. R., Balkanski, Y., Bauer, S.,
552 Berntsen, T., Bond, T. C., Boucher, O., Chin, M., Clarke, A., De Luca, N., Dentener, F.,
553 Diehl, T., Dubovik, O., Easter, R., Fahey, D. W., Feichter, J., Fillmore, D., Freitag, S., Ghan,
554 S., Ginoux, P., Gong, S., Horowitz, L., Iversen, T., Kirkevåg, A., Klimont, Z., Kondo, Y.,
555 Krol, M., Liu, X., Miller, R., Montanaro, V., Moteki, N., Myhre, G., Penner, J. E., Perlwitz,
556 J., Pitari, G., Reddy, S., Sahu, L., Sakamoto, H., Schuster, G., Schwarz, J. P., Seland, O.,
557 Stier, P., Takegawa, N., Takemura, T., Textor, C., van Aardenne, J. A., Zhao, Y.: Evaluation
558 of black carbon estimations in global aerosol models, *Atmos. Chem. and Phys.*, 9, 9001-9026,
559 2009.

560 Koehler, K. A., DeMott, P. J., Kreidenweis, S. M., Popovicheva, O. B., Petters, M. D., Carrico, C.
561 M., Kireeva, E. D. Khokhlova, T. D., Shonija, N. K.: Cloud condensation nuclei and ice
562 nucleation activity of hydrophobic and hydrophilic soot particles, *Phys. Chem. Chem. Phys.*,
563 11, 7906-7920, 2009.

564 Lamarque, J. F., Bond, T. C., Eyring, V., Granier, C., Heil, A., Klimont, Z., Lee, D., Liousse, C.,
565 Mieville, A., Owen, B., Schultz, M. G., Shindell, D., Smith, S. J., Stehfest, E., Van Aardenne,
566 J., Cooper, O. R., Kainuma, M., Mahowald, N., McConnell, J. R., Naik, V., Riahi, K., van
567 Vuuren, D. P.: Historical (1850-2000) gridded anthropogenic and biomass burning emissions
568 of reactive gases and aerosols: methodology and application, *Atmos. Chem. and Phys.*, 10
569 (15), 7017-7039, 2010.

570 Law, K. S., Stohl, A.: Arctic Air Pollution: Origins and Impacts, *Science*, 315 (5818), 1537-1540,
571 2007.

572 Liggio, J., Li, S.-M.: Organosulfate formation during the uptake of pinonaldehyde on acidic sulfate
573 aerosols, *Geophys. Res. Lett.*, 33, L13808, doi: 10.1029/2006GL026079, 2006.

574 Lubin, D., Simpson, A. S.: The longwave emission signature of urban pollution – radiometric FTIR
575 measurement, *Geophys. Res. Lett.*, 21 (1), 37-40, 1994.

576 Mareckova, K., R. Wankmueller, M. Anderl, B. Muik, S. Poupa, Wieser, M.: Inventory review
577 2008: Emission data reported under the LRTAP convention and NEC directive status of
578 gridded data, Technical report, EMEP Centre on Emission Inventories and Projections,
579 Vienna, 2008.

580 Nguyen, Q. T., Skov, H., Sørensen, L. L., Jensen, B., Grube, A., Massling, A., Glasius, M.,
581 Nøjgaard, J. K.: Source apportionment of particles at Station Nord, North East Greenland
582 during 2008-2010 using COPREM and PMF analysis, *Atmos. Chem. and Phys.*, 13, 35-49,
583 2013.

584 Petzold, A., Kopp, C., Niessner, R.: The dependence of the specific attenuation cross-section on
585 black carbon mass fraction and particle size, *Atmos. Environ.*, 31 (5), 661-672, 1997.

586 Petzold, A., Kramer, H., Schönlinner, M.: Continuous measurement of atmospheric black carbon
587 using a multi-angle absorption photometer, *Environ. Sci. and Pollut. Res.*, 4, 78-82, 2002.

588 Petzold, A., Schönlinner, M.: Multi-angle absorption photometry - a new method for the
589 measurement of aerosol light absorption and atmospheric black carbon, *J. Aerosol Sci.*, 35,
590 421-441, 2004.

591 Petzold, A., Ogren, J. A., Fiebig, M., Laj, P., Li, S. M., Baltensperger, U. Holzer-Popp, T., Kinne, S.,
592 Pappalardo, G., Sugimoto, N.: Recommendations for reporting “black carbon” measurements,
593 *Atmos. Chem. and Phys.*, 13 (16), doi: 10.5194/acp-13-8365-2013, 2013.

594 Quinn, P. K., Bates, T. S.: The case against climate regulation via oceanic phytoplankton sulphur
595 emissions, *Nature*, 480, 51-56, 2011.

596 Quinn, P. K., Bates, T. S., Baum, E., Doubleday, N., Fiore, A. M., Flanner, M., Fridlind, A.,
597 Garrett, T. J., Koch, D., Menon, S., Shindell, D., Stohl, A., Warren, S. G.: Short-lived
598 pollutants in the Arctic: their climate impact and possible mitigation strategies, *Atmos. Chem.*
599 *and Phys.*, 8, 1723-1735, 2008.

600 Raatz, W. E., and G. E. Shaw: Long-range tropospheric transport of pollution aerosols into the
601 Alaskan Arctic, *J. Clim. Appl. Meteorol.*, 23, 1052–1064, 1984.

602 Roberts, D. L., Jones, A.: Climate sensitivity to black carbon aerosol from fossil fuel combustion ,
603 *J. Geophys. Res- Atmos.*, 109, D16202, doi: 10.1029/2004JD004676, 2004.

604 Seinfeld, J. H., Pandis, S. N.: Atmospheric chemistry and physics: from air pollution to climate
605 change, 2nd edition, Wiley-Interscience, New York, 2006.

606 Sharma, S., Andrews, E., Barrie, L. A., Ogren, J. A., Lavoue, D.: Variations and sources of the
607 equivalent black carbon in the high Arctic revealed by long-term observations at Alert and
608 Barrow: 1989-2003, *J. Geophys. Res.-Atmos.*, 111, D14208, doi: 10.1029/2005JD006581,
609 2006.

610 Sharma, S., Brook, J. R., Cachier, H., Chow, J., Lu, G.: Light absorption and thermal measurements
611 of black carbon in different regions of Canada, *J. Geophys. Res.*, 107, 4771, doi:
612 10.1029/2002JD002496, 2002.

613 Sharma, S., Ishizawa, M., Chan, D., Lavoue, D., Andrews, E., Eleftheriadis, K., Maksyutov, S.: 16-
614 year simulation of Arctic black carbon: Transport, source contribution, and sensitivity
615 analysis on deposition, *J. Geophys. Res.-Atmos.*, 118, 2, 943-964, doi:
616 10.1029/2012JD017774, 2013.

617 Sharma, S., Lavoue, D., Cachier, H., Barrie, L. A., Gong, S. L.: Long-term trends of the black
618 carbon concentrations in the Canadian Arctic, *J. Geophys. Res.-Atmos.*, 109, D15203, doi:
619 10.1029/2003JD004331, 2004.

620 Simpson, D., Benedictow, A., Berge, H., Bergström, R., Emberson, L. D., Fagerli, H., Flechard, C.
621 R., Hayman, G. D., Gauss, M., Jonson, J. E., Jenkin, M. E., Nyíri, A., Richter, C., Semeena, V.
622 S., Tsyro, S., Tuovinen, J.-P., Valdebenito, Á., and Wind, P.: The EMEP MSC-W chemical
623 transport model – technical description, *Atmos. Chem. Phys.*, 12, 7825-7865, doi:
624 10.5194/acp-12-7825-2012, 2012.

625 Skov, H., Wahlin, P., Christensen, J., Heidam, N. Z., Petersen, D.: Measurements of elements,
626 sulphate and SO₂ in Nuuk Greenland, *Atmos. Environ.*, 40, 4775-4781, 2006.

627 Slinn, W.G.N.: Predictions for particle deposition to vegetative surfaces, *Atmos. Environ.*, 16,
628 1785-1794, 1982.

629 Slinn, S.A. and Slinn, W.G.N.: Predictions for particle deposition on natural waters, *Atmos.*
630 *Environ.*, 14, 1013-1026, 1980.

631 Stohl, A.: Characteristics of atmospheric transport into the Arctic troposphere, *J. Geophys. Res.*,
632 111, D11306, doi: 10.1029/2005JD006888, 2006.

633 Stohl, A., Berg, T., Burkhardt, J. F., Fjaeraa, A. M., Forster, C., Herber, A., Hov, O., Lunder, C.,
634 McMillan, W. W., Oltmans, S., Shiobara, M., Simpson, D., Solberg, S., Stebel, K., Strom, J.,
635 Torseth, K., Treffeisen, R., Virkkunen, K., Yttri, K. E.: Arctic smoke - record high air
636 pollution levels in the European Arctic due to agricultural fires in Eastern Europe in spring

637 2006, *Atmos. Chem. and Phys.*, 7, 511-534, 2007.

638 Stohl, A., Klimont, Z., Eckhardt, S., Kupiainen, K., Shevchenko, V. P., Kopeikin, V. M.,
639 Novigatsky, A. N.: Black carbon in the Arctic: the underestimated role gas flaring and
640 residential combustion emissions, *Atmos. Chem. and Phys.*, 13 (17), 8833-8855, doi:
641 10.5194/acp-13-8833-2013, 2013.

642 Strand, A., Hov, O.: A 2-Dimensional Global Study of Tropospheric Ozone Production, *J. Geophys.*
643 *Res.-Atmos.*, 99, 22877-22895, 1994.

644 Surratt, J. D., Kroll, J. H., Kleindienst, T. E., Edney, E. O., Claeys, M., Sorooshian, A., Ng, N. L.,
645 Offenberg, J. H., Lewandowski, M., Jaoui, M., Flagan, R. C., Seinfeld, J. H.: Evidence for
646 organosulfates in secondary organic aerosol, *Environ. Sci. and Technol.*, 41 (2), 517-527,
647 2007.

648 Swietlicki, E., Hansson, H.-C., Hämeri, K., Svenningsson, B., Massling, A., McFiggans, G.,
649 McMurry, P. H., Petäjä, T., Tunved, P., Gysel, M., Topping, D., Weingartner, E.,
650 Baltensperger, U., Rissler, J., Wiedensohler, A., Kulmala, M.: Hygroscopic properties of sub-
651 micrometer atmospheric aerosol particles measured with H-TDMA instruments in various
652 environments – a review, *Tellus B*, 60 (3), 432-469, 2008.

653 Vignati, E., Karl, M., Krol, M., Wilson, J., Stier, P., Cavalli, F.: Sources of uncertainties in
654 modelling black carbon at the global scale, *Atmos. Chem. and Phys.*, 10, 2595-2611, 2010.

655 Wang, Q., Jacob, D. J., Fisher, J. A., Mao, J., Leibensperger, E. M., Carouge, C. C., Le Sager, P.,
656 Kondo, Y., Jimenez, J. L., Cubison, M. J., Doherty, S. J.: Sources of carbonaceous aerosols
657 and deposited black carbon in the Arctic in winter-spring: implications for radiative forcing,
658 *Atmos. Chem. Phys.*, 11, 12453-12473, 2011.

659 van der Werf, G. R., Randerson, J. T., Giglio, L., Collatz, G.J., Mu, M., Kasibhatla, P. S., Morton,
660 D. C., DeFries, R. S., Jin, Y.: Global fire emissions and the contribution of deforestation,
661 savanna, forest, agricultural, and peat fires (1997-2009), *Atmos. Chem. and Phys.*, 10 (23),
662 11707-11735, 2010.

663 Yttri, K. E., Myhre, C. L., Eckhardt, S., Fiebig, M., Dye, C., Hirdman, D., Stroem, J., Klimont, Z.,
664 Stohl, A.: Quantifying black carbon from biomass burning by means of levoglucosan - a one-
665 year time series at the Arctic observatory Zeppelin, *Atmos. Chem. and Phys.*, 14 (12), 6427-
666 6442, 2014.

667

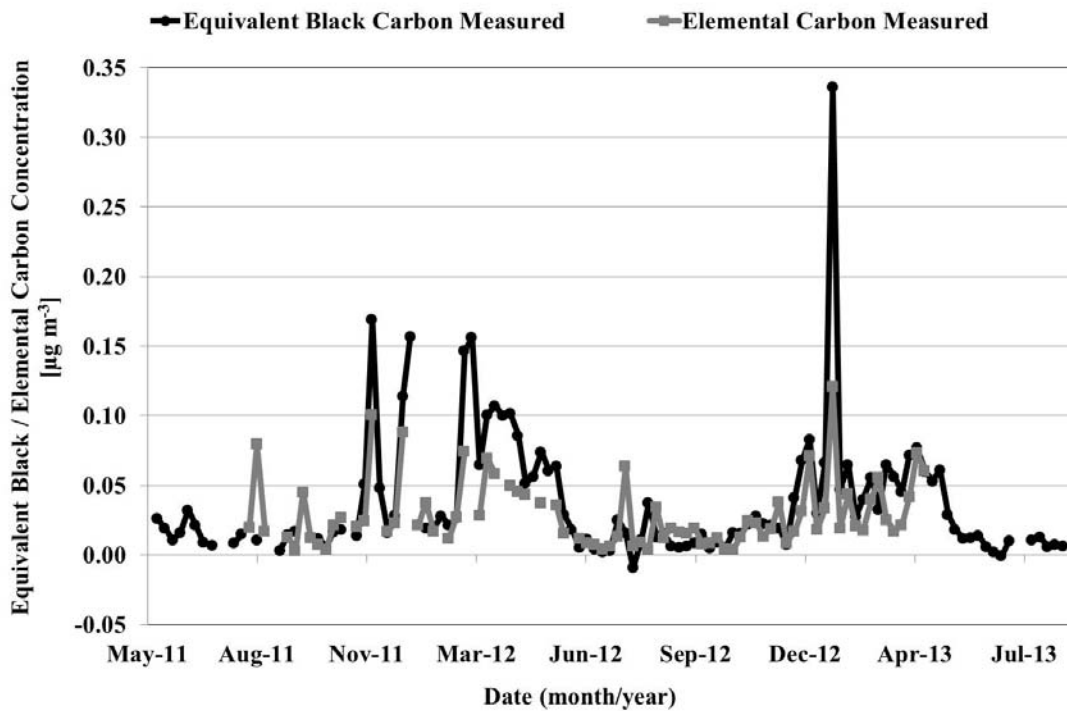
668 **Tables**

669 **Table 1:** Mean measured and modeled EBC/BC and sulfate concentrations together with mean
 670 measured EC and OC concentrations during the different seasons at VRS (Station Nord), North
 671 Greenland between May 2011 and August 2013.

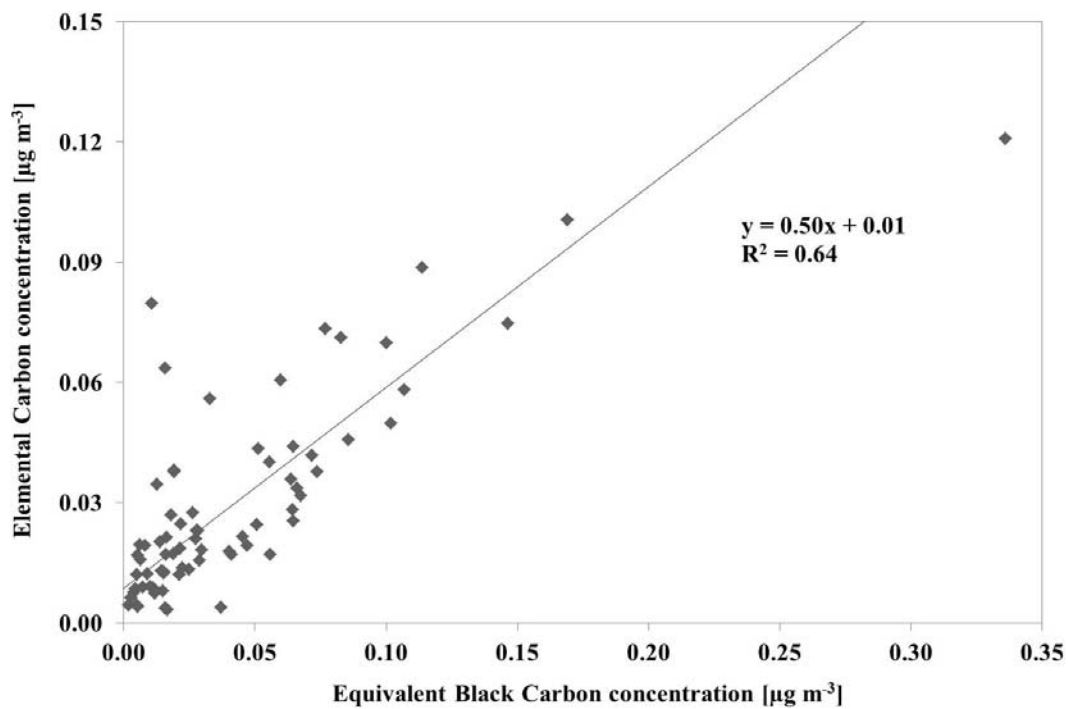
	<i>EBC measured</i> [$\mu\text{g m}^{-3}$]	<i>Sulfate measured</i> [$\mu\text{g m}^{-3}$]	<i>BC modeled</i> [$\mu\text{g m}^{-3}$]	<i>Sulfate modeled</i> [$\mu\text{g m}^{-3}$]	<i>EC measured</i> [$\mu\text{g m}^{-3}$]	<i>OC measured</i> [$\mu\text{g m}^{-3}$]
Summer (June, July, August)	0.011 +/- 0.009	0.112 +/- 0.072	0.019 +/- 0.013	0.144 +/- 0.097	0.020 +/- 0.022	0.151 +/- 0.079
Autumn (September, October, November)	0.022 +/- 0.034	0.138 +/- 0.120	0.011 +/- 0.015	0.317 +/- 0.398	0.019 +/- 0.020	0.144 +/- 0.077
Winter (December, January, February)	0.067 +/- 0.071	0.485 +/- 0.397	0.040 +/- 0.033	0.900 +/- 0.657	0.036 +/- 0.028	0.202 +/- 0.149
Spring (March, April, May)	0.054 +/- 0.029	0.480 +/- 0.243	0.022 +/- 0.017	0.618 +/- 0.582	0.042 +/- 0.018	0.245 +/- 0.061
Total no. of samples	106	94	119	119	78	78

672

673 **Figure Captions**

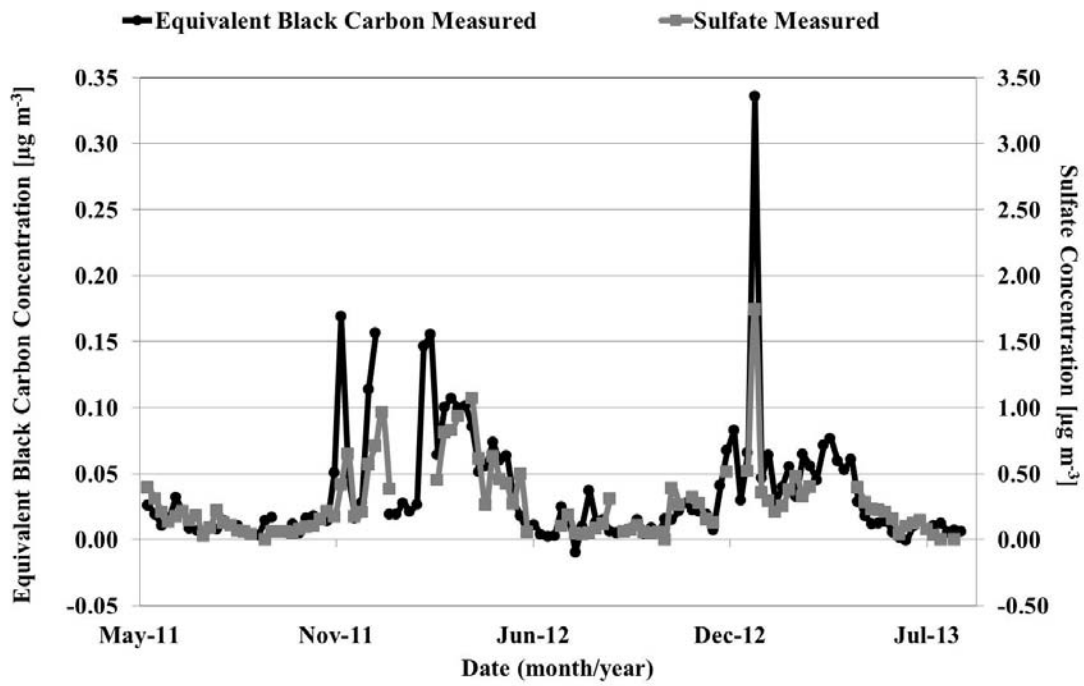


674
675 a)

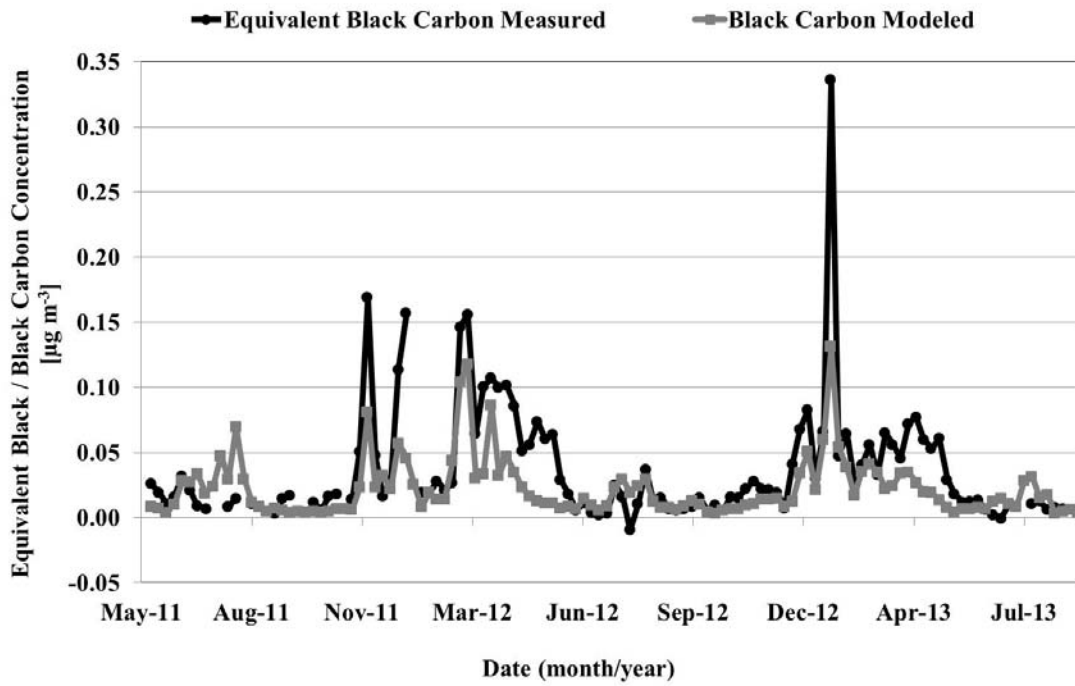


676
677 b)

678 **Figure 1:** a) Weekly measured EBC and EC concentrations in $\mu\text{g m}^{-3}$ from May 2011 to August
679 2013 at VRS (Station Nord), North Greenland. Both EBC and EC show the same seasonal variation
680 with maximum concentrations in winter and spring and minimum concentrations in summer, b)
681 scatter plot of measured EC and EBC concentrations (the slope obtained by orthogonal regression is
682 $y = 0.50$ showing a correlation coefficient of $R^2 = 0.64$).

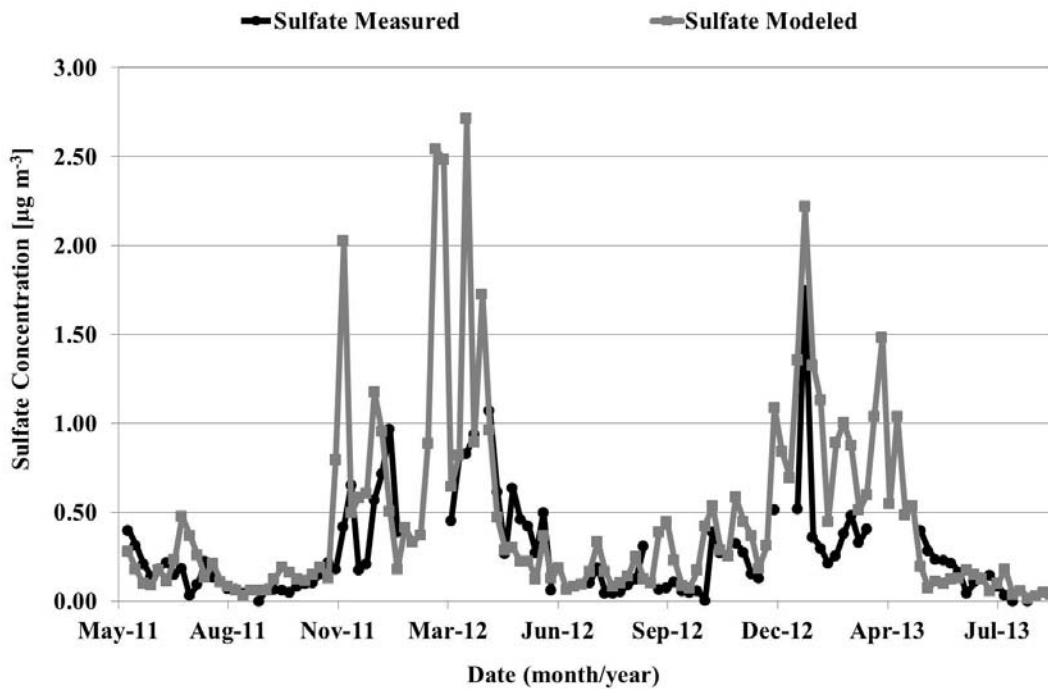


683
 684 **Figure 2:** Weekly measured EBC and sulfate concentrations in $\mu\text{g m}^{-3}$ from May 2011 to August
 685 2013 at VRS (Station Nord), North Greenland. Here, EBC and sulfate concentrations exhibit very
 686 similar patterns with maximum concentrations in winter and spring compared to minimum
 687 concentrations in summer.
 688



689
690
691

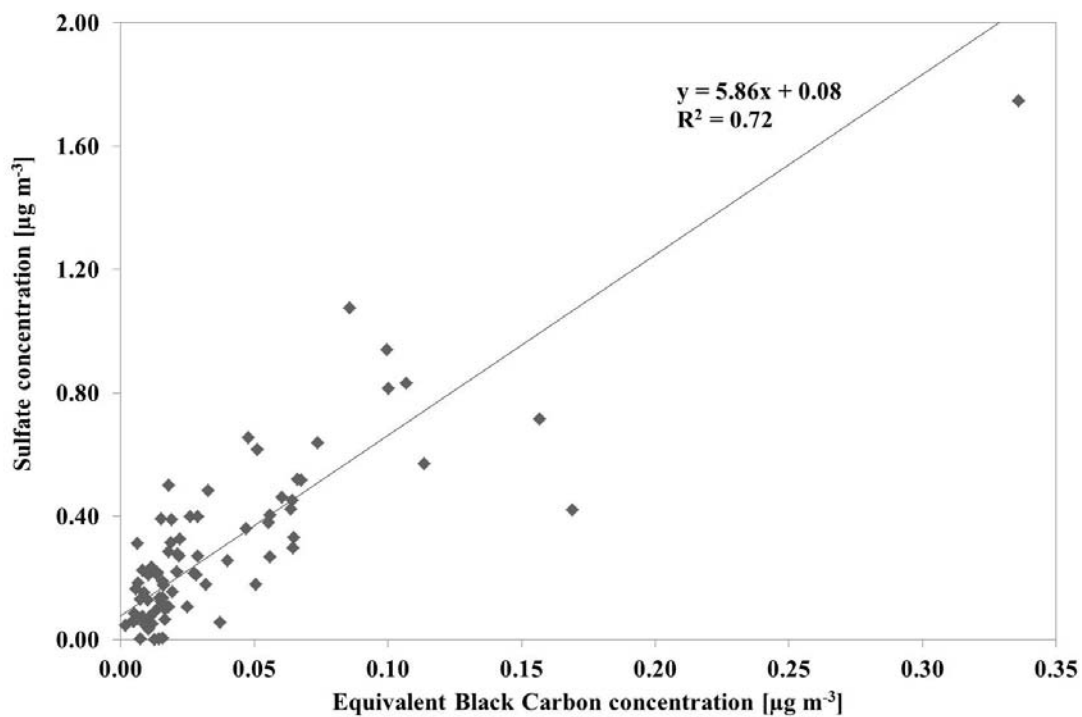
a)



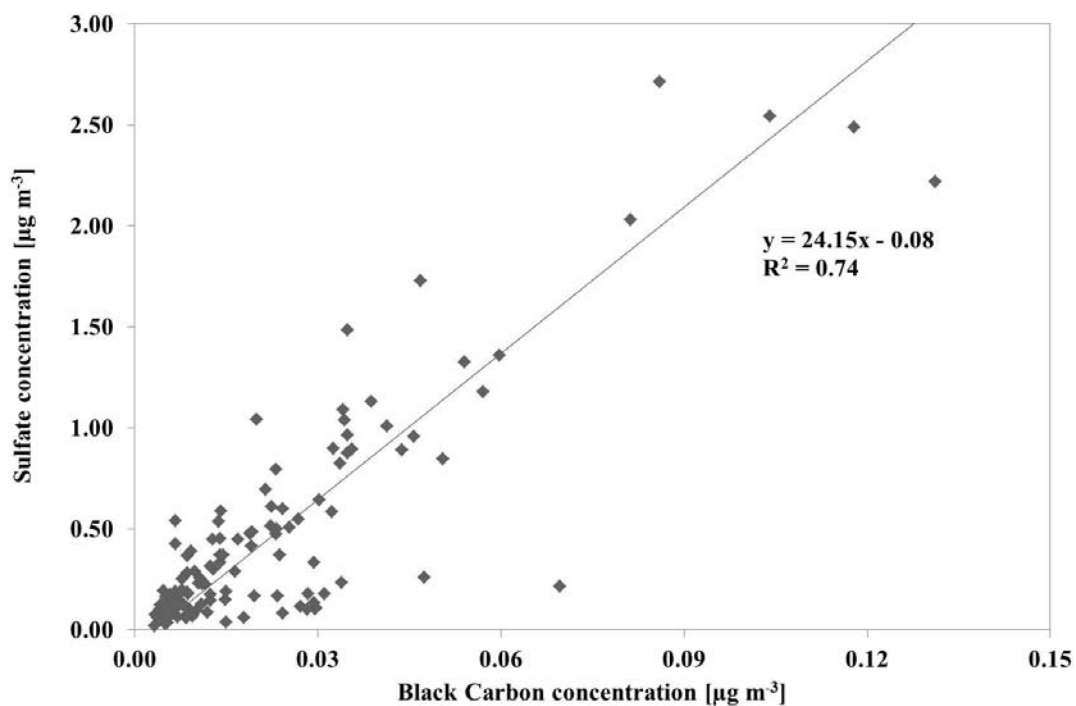
692
693

b)

694 **Figure 3:** Comparison of measurement and model results from DEHM for (a) EBC/BC and (b)
695 sulfate concentrations at VRS (Station Nord), North Greenland, during the time period from May
696 2011 to August 2013.



697
698 a)



699
700 b)

701 **Figure 4:** Scatter plot of EBC/BC and sulfate concentrations based on (a) measurement results (the
702 slope obtained by orthogonal regression between sulfate and EBC is $y = 5.86$ showing a correlation
703 coefficient of $R^2 = 0.72$) and (b) model results (the slope obtained by orthogonal regression between
704 sulfate and BC is $y = 24.15$ showing a correlation coefficient of $R^2 = 0.74$) during May 2011 to
705 August 2013 at VRS (Station Nord), North Greenland.